Robotica: (2020) volume 38, pp. 1381–1399. © Cambridge University Press 2019
doi:10.1017/S0263574719001528

Evaluation of Topological Properties of Parallel Manipulators Based on the Topological Characteristic Indexes

Huiping Shen†*, Ting-Li Yang†, Ju Li†, Dan Zhang‡, Jiaming Deng† and Anxin Liu¶

†School of Mechanical Engineering, Changzhou University, Jiangsu 213164, China
E-mails: yangtl@126.com, wangju0209@163.com, czdydjm@126.com
‡Lassonde School of Engineering, York University, Toronto ON M3J1P3, Canada
E-mail: dzhang99@yorku.ca
¶Nanjing University of Aeronautics and Astronautics Nanhang Jincheng College, Jiangsu 211156, China
E-mail: liuanxinn@163.com

(Accepted October 9, 2019. First published online: November 19, 2019)

SUMMARY
The topological structure of a parallel manipulator (PM) determines its intrinsic topological properties (TPs). The TPs further determine essential kinematic and dynamic properties of the mechanism. TPs can be expressed through topological characteristics indexes (TCI). Therefore, defining a set of TCIs is an important issue to evaluate the TPs of PMs. This article addresses the evaluation of topological properties (ETP) of PMs based on TCI. A general and effective ETP method for PMs is proposed. Firstly, 12 TCIs are proposed, including 8 quantitative TCIs, that is, position and orientation characteristics sets (POC), dimension of the POC set, degrees of freedom (DOF), number of independent displacement equations, types and number of an Assur kinematic chain (AKC), coupling degrees of the AKCs, degrees of redundancy and the number of overs; as well as 4 qualitative TCIs, that is, selection of actuated joints, identification of inactive joints, DOF type and Input–Output motion decoupling. Secondly, the ETP method is illustrated by evaluating some well-known PMs including the Delta, Tricept, Exechon, Z3, H4 and the Gough–Stewart platform manipulators, as well as 28 other typical PMs. Via the ETP analysis of these mechanisms also some valuable design knowledge is derived and guidelines for the design of PMs are established. Finally, a 5-DOF decoupled hybrid spraying robot is developed by applying the design knowledge and the design guidelines derived from the ETP analysis.

KEYWORDS: Parallel manipulators; Evaluation of topological properties; Topological characteristics index; Position and orientation characteristics; Coupling degree; Single-opened-chain unit.

NOMENCLATURE

TP	Topological property
ETP	Evaluation of topological properties
TCI	Topological characteristics index
POC	Position and orientation characteristics
SOC	Ordered single-open-chain
HSOC	Hybrid-single-open-chain

* Corresponding author. E-mail: shp65@126.com

DOF	Degree of freedom
AKC	Assur kinematics chain with zero DOF
PM	Parallel manipulator or parallel mechanism or parallel kinematic mechanism (PKM)
I–O	decoupling Input–output motion decoupling
N	number of branches between the base and moving platform
M_{pa}	POC elements of the moving platform of a PM
M_{bj}	POC elements of the end link of the jth branch or limb
F	DOF of a mechanism
f_i	DOF of the ith joint
m	number of all joints in the whole mechanism
m_j	number of joints in jth M_{bj}
n	number of all links in the whole mechanism
v	number of all independent loops
ξ_{Lj}	number of an independent displacement equation of the jth loop
ξ	total number of independent displacement equations of the whole mechanism
I_j	number of actuated joints of jth SOC
D_{Re}	degree of redundancy
N_{ac}	number of actuated joint
Δ_j	constraint degree of jth SOC
k	coupling degree
T	translation
R	rotation

1. Introduction

Currently, there are several main methods for type synthesis of a parallel manipulator (PM). These are based on screw theory,[1,2] displacement subgroups,[3] linear transformations[4] and the position and orientation characteristics (POC) method.[5–8] A large number of PMs have been synthesized using these methods. However, only very few PMs such as the Delta, Tricept, Exechon, Z3, H4 and the Gough–Stewart manipulator are used by industry. Some of these manipulators have been designed based on intuition or practical innovation approaches rather than on the theoretical synthesis methods mentioned earlier. On the other hand, one has to confess that it is difficult to select a better PM solution through complex and time-consuming kinematic and dynamic analysis. This motivates researchers to derive useful design knowledge and guidelines by studying successful PMs that help them understand the topological properties (TPs) that are associated with the kinematic and dynamic performance of mechanisms. However, this research topic is still open, and only few methods for the evaluation of topological properties (ETP) have been reported in the literature to date. This article will address methods for the ETP of PMs based on topological characteristics indexes (TCI).

It is known that the topological structure of a PM determines its intrinsic TPs, while on the other hand TPs determine its essential kinematic and dynamic performance. TPs can be determined using different methods for the ETP analysis and can furthermore be expressed through TCI. The relations among the topological structure, TP, ETP and TCI of a mechanism are displayed in Fig. 1.

Thus, proposing a set of TCI is important to evaluate the TP of an existing PM to effectively perform a kinematic and dynamic analysis.

Three challenging issues, that is, the ETP, type classification and the optimization of PM design solutions, should be solved before performing the kinematic and dynamic analysis. The purpose of the ETP is to obtain the basic topological characteristics during the conceptual design phase to conduct effectively the kinematic and dynamic modeling. The significance of the ETP in the analysis and design of mechanisms is illustrated in Fig. 2.

Figure 2 shows the contribution of this article to the design development process of a new PM. The TPs (POC, degrees of freedom (DOF), type and number of AKC, k, etc.), together with the kinematic properties (position, velocity, acceleration, workspace, etc.) and the dynamic properties (force, torque, stiffness, etc.), make up the total performance of a mechanism. Therefore, ETP of existing PMs will help identify their TCIs to effectively perform kinematic and dynamic analysis, trajectory planning and motion control algorithm design.

The ETP of a new family of PMs with n-DOF $aTbR$ ($a+b=n$, $n=2\sim 6$, *T is for translation and R is for rotation*) will assist in the classification and optimization of their topological structure and,

https://doi.org/10.1017/S0263574719001528 Published online by Cambridge University Press

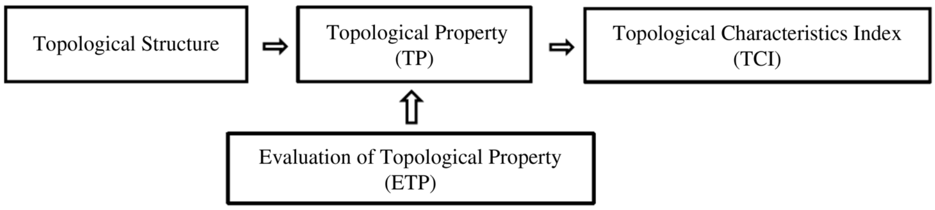

Fig. 1. Relations among topological structure, TP, ETP and TCI.

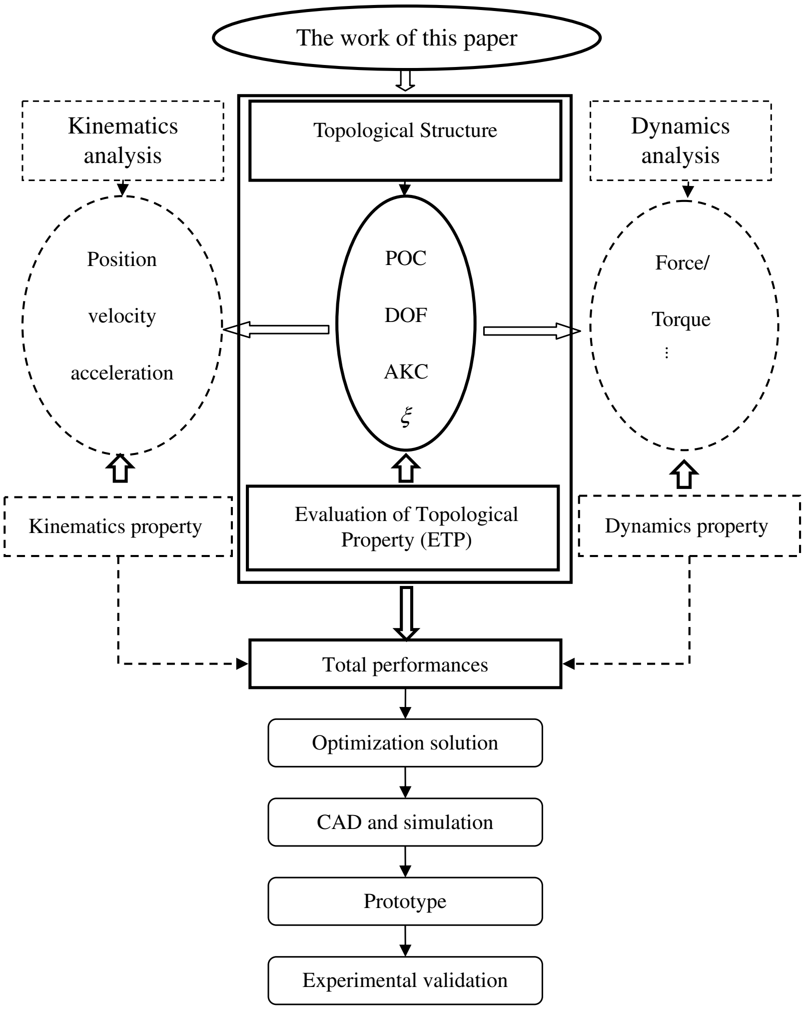

Fig. 2. Significance of ETP in mechanism analysis and design.

therefore, in the identification of most promising topological solutions. For example, for the family of 6-DOF 6-SPS Gough–Stewart platform manipulators and its derivatives, that is, the 1-1-1-1-1-1, 2-1-1-1-1, 2-2-2, 2-2-1-1, 3-1-1-1, 3-2-1 types, here, *1, 2 and 3, respectively, denote that there is single-, double- and triple-spherical joints at the moving platform*. We have calculated and proved that the coupling degrees k of six 6-SPS PMs are 3, 2, 1, 1, 1, 0, respectively.[9] We can, therefore, select those topological PMs having a low coupling degree such as the 2-2-2, 2-2-1-1, 3-1-1-1 types with $k = 1$ or the 3-2-1 type with $k = 0$, to easily perform forward kinematics while keeping their POC unchanged,[9,10] that is, a three-translation and three-rotation output of the moving platform. The coupling degree k will be addressed in Section 2.1 and Eq. (9). In addition, one could consider PMs with an input–output motion decoupling (I–O decoupling) property such as the 3-2-1 type to perform easily trajectory planning and motion control.

However, this article focuses mainly on ETP of existing PMs.

https://doi.org/10.1017/S0263574719001528 Published online by Cambridge University Press

Gogu *et al.*[4] defined four structural parameters to describe the performance characteristics of PMs, which include degrees of mobility, degrees of connectivity (spatiality), degrees of redundancy and number of overconstraints of the PMs.[4] Accordingly, four corresponding formulae are proposed.

Yang and his group members have established a new methodology for the topological structure design of PMs based on the POC equations,[5–8] the so-called POC method. The methodology includes three basic concepts (dimension constraint types, POC sets and ordered single-open-chain (SOC) units), one mechanism composition principle based on SOC units, four basic formulae (POC union equation for serial mechanisms, POC intersection equation for PMs, general DOF formula and coupling degree formula) and a procedure for type synthesis. Thirteen types of PMs, having 2-DOF to 6-DOF, that is, n-DOF$aTbR$ with $a+b=n$ and $n=2\sim 6$, have been synthesized using this methodology.[6] This methodology comprises simple mathematical operations, clear physical meaning and easy usage. By using this methodology non-instantaneous mechanisms that have unchanged DOF and POC during their continuous motion process could be obtained.

Based on this methodology, this article proposes a general ETP method that defines 12 TCIs of a PM, including 8 quantitative TCIs (i.e., POC sets, dimensions of the POC set, DOF, number of independent displacement equations, types and number of Assur kinematic chain (AKC), coupling degrees of AKC, degrees of redundancy and number of overconstraints), as well as 4 qualitative TCIs (i.e., selection of actuated joints, identification of inactive joints, identification of DOF type and identification of input–output motion decoupling). Moreover, the ETP analysis for some successful PMs is conducted including 6 well-known PMs and 28 typical PMs, which results in the intrinsic topological characteristics of these mechanisms and some valuable design insight as well as design guidelines that can be used in mechanism design.

The article is organized as follows. In Section 2 a general method for the ETP analysis of PMs is presented including their calculation formulae, the determination criteria and the physical meaning of the 12 TCIs. In Section 3 some important TCIs for each of the 6 well-known PMs and 28 typical PMs are obtained and analysed, respectively. Section 4 illustrates the conception and design of a novel 5-DOF decoupled hybrid spraying robot using the design knowledge of PMs and the related valuable design guidelines derived from ETP analysis conducted in the article. Conclusions are presented in Section 5.

2. The ETP Method for PMs

2.1. Theoretical basis of the ETP method

The ETP method proposed here involves the calculation of eight quantitative TCIs and the determination of four qualitative TCIs for PMs. The formulae of the eight quantitative TCIs are presented in next eight subsections (2.1.1–2.1.8), while the determination criteria of the four qualitative TCIs are explained in subsections 2.1.9–2.1.12. All the TCLs are illustrated in Figs. 5 and 6 and in Table I.

2.1.1. Type of POC sets. The types of POC sets can be obtained based on both the POC union operation equation for a serial limb and the POC intersection operation equation for a PM.

(a) POC union operation equation for a serial limb

The POC union operation equation for a serial limb is

$$M_S = \bigcup_{i=1}^{m} M_{J_i} = \bigcup_{j=1}^{k} M_{\text{sub}-\text{SOC}_j} \tag{1}$$

where M_S is the POC set of the end link of the limb related to the base, including both translational and rotational elements. m is the number of kinematic joints. M_{J_i} is the POC set of the ith joint. $M_{\text{sub}-\text{SOC}_j}$ is the POC set of the jth sub-SOC.

The symbol "$\bigcup$" stands for a union operation. Ten union operation rules for Eq. (1) include eight linear operation rules and two nonlinear criteria.[6]

https://doi.org/10.1017/S0263574719001528 Published online by Cambridge University Press

Table I. Twelve TCIs and their calculation formulae or criteria.

No.	**Topological characteristics index (TCI)**	**Formula or criteria**
1	Type of POC sets	$M_S = \bigcup_{i=1}^{m} M_{Ji} \quad M_{Pa} = \bigcap_{i=1}^{v+1} M_{bi}$
2	Dimension of the POC sets*	$\dim.\{M\} \leq \mathrm{DOF}$
3	DOF*	$F = \sum_{i=1}^{m} f_i - \sum_{j=1}^{v} \dim.\left\{\left(\bigcap_{i=1}^{j} M_{b_i}\right) \bigcup M_{b_{(j+1)}}\right\}$
4	Number of independent displacement equations	$\xi = \sum_{j=1}^{v} \dim.\left\{\left(\bigcap_{i=1}^{j} M_{b_i}\right) \bigcup M_{b_{(j+1)}}\right\}$
5	Types and number of AKCs	$\mathrm{AKC} = \sum_{j=1}^{v} \mathrm{SOC}_j$
6	Coupling degrees of an AKC	$k = {}^1\!/_2 \min\left\{\sum_{j=1}^{v} \lvert\Delta_j\rvert\right\}$
7	Degrees of redundancy*	$D_{Re} = N_{ac.} - \dim.(M)$
8	Number of overconstraints*	$N_{\mathrm{ov.}} = 6v - \xi$
9	Selection of actuated joints	Criterion for selection of actuated joints
10	Identification of inactive joints	Criterion for identification of inactive joints
11	Identification of the DOF types	Criterion for identification of the DOF type
12	Identification of I–O decoupling	Criterion for identification of I–O decoupling

No. 1, *No. 4*, *No. 5*, *No. 6 and No. 9 ˜ No. 12* in Fig. 5 and Table I are proposed as new TCIs by the authors in this article. The other four TCIs with asterisk "*", *No. 2*, *No. 3*, *No. 7 and No. 8*, are similar to the four structure parameters proposed by Gogu *etal.* that are used to describe performance characteristics of PMs.[4]

(b) POC intersection operation equation for a PM

The POC intersection operation equation for a PM is

$$M_{Pa} = \bigcap_{j=1}^{(v+1)} M_{b_j} \tag{2}$$

where M_{Pa} is the POC set of the moving platform of a PM. M_{b_j} are the POC sets of the end link in the jth branch (limb). v is the number of independent loops.

The symbol "$\bigcap$" stands for an intersection operation. There are 12 intersection operation rules for Eq. (2), including ten linear operation rules and two nonlinear criteria.[6]

According to Eq. (2), there is

$$M_{b_j} \supseteq M_{Pa} \tag{3}$$

Here the symbol "$\supseteq$" means including, that is, the POC set elements of the end link in the jth branch, M_{b_j}, must contain the POC set elements of the moving platform of a PM, that is, M_{Pa}.

2.1.2. Dimension of the POC sets. The number of independent translational and rotational elements in the POC sets should be less than or equal to (i.e., not be greater than) the number of DOF of the PM, that is,

$$\dim\{M\} = \dim\{M(r)\} + \dim\{M(t)\} \leq F \tag{4}$$

where F is the number of DOF of the PM, $\dim\{M\}$ is the dimension of the POC sets (namely, number of its independent elements). $\dim\{M(t)\}$ is the number of independent translational elements $t(\dim\{M(t)\} = 0, 1, 2 \text{ or } 3)$, and $\dim\{M(r)\}$ is the number of independent rotational elements $r\ (\dim\{M(r)\} = 0, 1, 2 \text{ or } 3)$.

For example in Fig. 3 is a 3-DOF planar 8-bar mechanism. Its independent elements (two translational and one rotational) in the POC sets of the moving platform are three, and the number of DOF is also three, that is, $\dim.\{M_{Pa}\} = 3 = DOF$. However, in Fig. 4 a 5-DOF planar 10-bar mechanism is displayed. Its independent elements (two translational and one rotational) in the POC sets of the moving platform are still three, but the number of DOF is five. Therefore, we have $\dim.\{M_{Pa}\} = 3 < \mathrm{DOF} = 5$.

2.1.3. DOF. A general DOF formula based on motion analysis is given as follows, from which one can obtain a full-cycle DOF instead of an instantaneous DOF of a mechanism.[8,11]

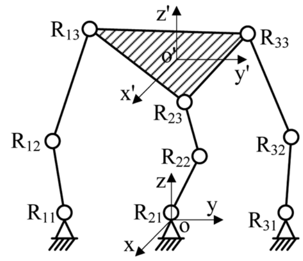

Fig. 3. A 3-DOF planar 8-bar mechanism. Note: The dimension of the POC set in this article is actually the degree of connectivity (or spatiality).[4]

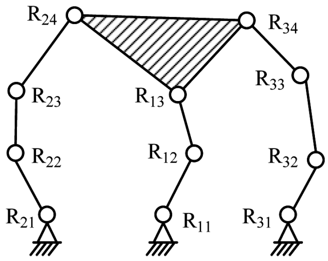

Fig. 4. A 5-DOF planar 10-bar mechanism. Note: The dimension of the POC set in this article is actually the degree of connectivity (or spatiality).[4]

$$F = \sum_{i=1}^{m} f_i - \sum_{j=1}^{v} \xi_{L_j} \tag{5a}$$

$$\xi_{L_j} = \dim . \left\{ \left(\bigcap\nolimits_{j=1}^{j} M_{b_j} \right) \bigcup M_{b_{(j+1)}} \right\} \tag{5b}$$

Here, f_i is the number of DOF of the ith joint, ξ_{L_j} is the number of independent displacement equations for the jth loop. The so-called full-cycle DOF means that the mechanism has an unchanged DOF during its motion process, whereas the instantaneous DOF means that the mechanism has a changing DOF during its motion process.

2.1.4. Number of independent displacement equations. The number of independent displacement equations can be obtained as follows[8,11]

$$\xi = \sum_{j=1}^{v} \dim . \left\{ \left(\bigcap\nolimits_{i=1}^{j} M_{b_i} \right) \bigcup M_{b_{(j+1)}} \right\} \tag{6}$$

The number of independent displacement equations indicates the constraint influence of each independent loop on the PM.

Note: In order to get the DOF, Eq. (6) should be applied before Eq. (5).

2.1.5. Types and number of an AKC. According to the mechanism composition principle based on the SOCs,[7,8] any kinematic chain can be decomposed into v ordered SOC $i(i = 1, 2, \ldots, v)$. The constraint degree Δ_i $(i = 1, 2, \ldots, v)$ of each SOC i can be obtained. Then combine SOCs having the constraint degrees delta_1, delta_2, into several groups and ensure that the sum of each group is zero. Then, each group represents an AKC with zero DOF. Therefore, any kinematic chain can be decomposed into several AKCs. It should be noted that the decomposition is not necessarily unique. The decomposition process can be expressed as follows:

$$\mathrm{KC}[F, v] = \sum \mathrm{SOC}_j(\Delta_j) = F - J_{\mathrm{in}} + \sum \mathrm{AKC}_i[v_i, k_i] \tag{7}$$

https://doi.org/10.1017/S0263574719001528 Published online by Cambridge University Press

where KC[F, v] is a kinematic chain with F DOFs and v independent loops, AKC$_i$[v_i, k_i] represents the ith AKC with independent loops of v_i and coupling degree of k_i. $F - J_{\text{in}}$ means F joints of input. The constraint degree of the jth SOC is defined as follows

$$\Delta_j = \sum_{i=1}^{m_j} f_i - I_j - \xi_{L_j} = \begin{cases} \Delta_j^- = -5, -4, -3, -2, -1. \\ \Delta_j^0 = 0 \\ \Delta_j^+ = +1, +2, +3, \cdots \end{cases} \tag{8}$$

Here I_j is the number of actuated joints in the SOC$_j$. The notation of m_j, f_i ξ_{L_j} has been defined before.

2.1.6. Coupling degree of an AKC. From Eq. (7), we know that an AKC can be decomposed into several SOCs in various ways. Then, the coupling degree k of an AKC is defined as[6,8]

$$k = \left|\Delta_j^-\right| = \Delta_j^+ = \frac{1}{2} \min \left\{ \sum_{j=1}^{v} \left|\Delta_j\right| \right\} \tag{9}$$

Here, min{•} operation means that the decomposition sequence with the smallest $\sum_{j=1}^{v} \left|\Delta_j\right|$ should be selected.

The constraint degree Δ_j of the jth SOC indicates the constraint influences of the chain on the kinematic performance of the mechanism. Its physical meaning will be explained next:

(a) An SOC with negative constraint degree, denoted as SOC(Δ_j^-), will apply $\left|\Delta_j^-\right|$ constraint equations to a mechanism and the number of DOF of the mechanism will be decreased by $\left|\Delta_j^-\right|$ DOFs.
(b) An SOC with positive constraint degree, denoted as SOC(Δ_j^+), will increase the number of DOF of the mechanism by Δ_j^+. Therefore, its forward kinematics solutions could not be solved immediately. Its assembly can be determined only on the condition that Δ_j^+ virtual variables are assigned. When the number of the virtual variables is equal to the number of $\left|\Delta_j^-\right|$ constraint equations applied in SOC(Δ_j^-), that is, $k = \left|\Delta_j^-\right| = \Delta_j^+$, the motion of the mechanism is defined and its forward kinematics can be obtained.
(c) An SOC with zero constraint degree, denoted as SOC(Δ_j^0), does not affect the DOF. Its forward kinematics solutions can be obtained immediately without assigning virtual variables.

Therefore, the coupling degree k describes the complexity level of the topological structure of a PM, and it also represents the complexity level of its kinematic and dynamic analysis. The lower the coupling degree k, the easier is the treatment of its forward kinematic and dynamic analysis is.[7,10]

2.1.7. Degrees of redundancy. The degree of redundancy of a PM is defined as

$$D_{\text{Re}} = N_{\text{ac.}} - \dim\{\text{M}\} \tag{10}$$

where N_{ac} is the number of actuated joints.

2.1.8. Number of overconstraints. The number of overconstraints is defined as

$$N_{\text{ov}} = 6v - \xi \tag{11}$$

where ξ is the sum of the number of independent displacement equations of the whole mechanism, which can be obtained from Eq. (6). v is the number of independent loops.

2.1.9. Selection of the actuated joints. The selection of the actuated joints should comply with the criterion proposed next:

Pre-selecting F joints in an F-DOF mechanism as actuated joints and fixing these joints will lead to a new mechanism or structure. If the number of DOF of the new mechanism or structure is $F^* = 0$,

https://doi.org/10.1017/S0263574719001528 Published online by Cambridge University Press

these pre-selected F joints can be used as actuated joints. If $F^* > 0$, these F pre-selected joints cannot be used as actuated joints.

2.1.10. Identification of inactive joints. The notion inactive joint stands for a negative (or passive or hypocritical) joint that does not work during the motion process of a PM, meaning that it looks like a joint but it is actually static, whereas active joint means joints that are movable, including actuated or non-actuated joints. Therefore, identification of inactive joint(s) in a PM is important for the designer to simplify the mechanism's topological structure as the inactive joints could be deleted. In the following an effective algorithm to identify inactive joints will be presented.

For a mechanism whose number of DOF > 0, we assume that a certain chosen joint is fixed, which will lead to a new mechanism or a structure. If the number of DOF of the original mechanism is equal to that of the new mechanism or the structure, the fixed joint must have been an inactive joint. Otherwise, it is the active joint.

2.1.11. Identification of DOF types. To address the I–O motion decoupling properties, three types of DOF are defined: the complete DOF, the incomplete DOF and the separate DOF. For an arbitrary multi-DOF mechanism the identification criteria for the different DOF types are given as follows:

(a) When a mechanism contains only one AKC and all actuated joints of the mechanism are located in this AKC, that is, each position output element or orientation output element, that is, $(x, y, z, \alpha, \beta, \gamma)$, is a function of all actuated joints $(\theta_1, \cdots, \theta_F)$ that are located in this AKC, we define the mechanism to have a complete DOF.
(b) When a mechanism contains several AKCs and the actuated joints of the mechanism are located in different AKCs, respectively, that is, each position output element or orientation output element is a function of some actuated joints, that is, $(\theta_1, \cdots, \theta_u)(u < F)$, that are located in different AKCs, we define the mechanism to have an incomplete DOF.
(c) When a mechanism contains several AKCs and the actuated joints of the mechanism are located in different AKCs, respectively, moreover the mechanism can be decomposed into several separate sub-mechanisms by cutting the frame, and a sub-mechanism may have one AKC or several AKCs, we define the mechanism to have a separate DOF.

2.1.12. Identification of the input–output motion decoupling. According to the identification criteria of the DOF types stated earlier, the input–output motion decoupling detection, that is, I–O decoupling, can be addressed as follows:[6]

(a) If each position and orientation output element $(x, y, z, \alpha, \beta, \gamma)$ is a function of all actuated joints $(\theta_1, \cdots, \theta_F)$, then the input–output motion is not decoupled. Therefore, the mechanism is not I–O decoupled when it has a complete DOF.
(b) If some position or orientation output elements are a function of only some actuated joints $(\theta_1, \cdots, \theta_u)(u < F)$, then the input–output motion is partially decoupled. Therefore, the mechanism is partially I–O decoupled when it has an incomplete DOF.
(c) If there is a one-to-one relation between the input and the output as shown in Eq. (12a), or if there is a "triangle" relation between the inputs and the outputs as shown in Eq. (12b), then the input–output motion is decoupled. Therefore, the mechanism is I–O decoupled when it has separate DOF.

$$M_{Pa} = \begin{bmatrix} x(\theta_1) & y(\theta_2) & z(\theta_3) \\ \alpha(\theta_4) & \beta(\theta_5) & \gamma(\theta_6) \end{bmatrix} \tag{12a}$$

$$M_{Pa} = \begin{bmatrix} x(\theta_1) & y(\theta_1, \theta_2) & z(\theta_1 \sim \theta_3) \\ \alpha(\theta_1 \sim \theta_4) & \beta(\theta_1 \sim \theta_5) & \gamma(\theta_1 \sim \theta_6) \end{bmatrix} \tag{12b}$$

If the input–output motion of a mechanism is decoupled, its kinematic and dynamic analysis and the trajectory planning and the motion control are simplified. Type synthesis of I–O decoupled PMs

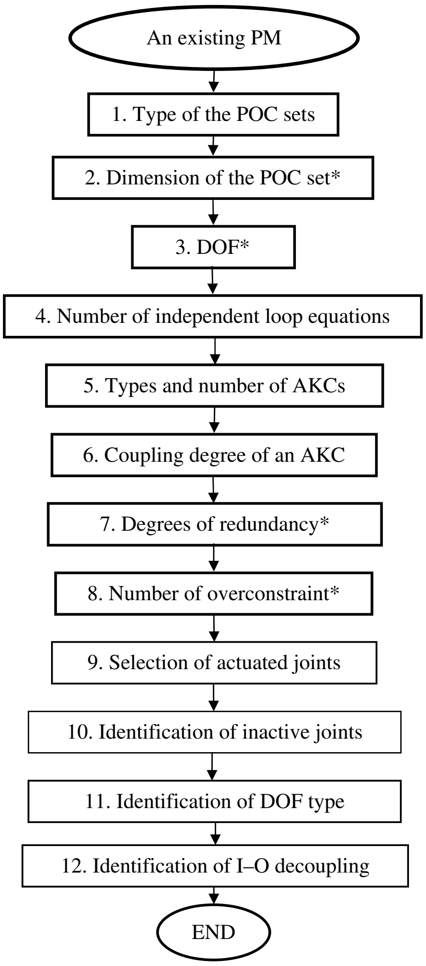

Fig. 5. A general flowchart of ETP analysis for an existing PM.

has gained considerable attention.[4,12–15] However, based on previous work on PMs,[9] the authors consider the I–O decoupling property as 1 of the 12 TCIs in the ETP analysis, and moreover suggest that I–O decoupling analysis should become an important step before performing kinematic analysis, trajectory planning and designing motion control for a mechanism. This is due to the fact that I–O decoupling analysis will assist in the identification of promising PM solutions with easier trajectory planning and motion control during the conceptual design phase.

Thus, a generic flowchart of the procedures for ETP of PMs is given in Fig. 5, which suggests a basic sequence of the ETP analysis.

It is noted that the *No. 1* ∼ *No. 8* eight quantitative TCIs in Fig. 5 have been implemented in an automatic computer-aided analysis programme based on a set of algorithms that we have developed.[12] The programme will be an efficient tool to perform ETP analysis for those mechanism designers who are not very familiar with the ETP method.

The calculation formulae for the eight quantitative TCIs and the determination criteria for four qualitative TCIs of the ETP analysis are summarized in Table I.

2.2. *Physical meaning of the 12 TCIs*

The 12 TCIs represent the intrinsic and essential topological properties of a PM that are associated with the kinematic and dynamic performance of the PM. The physical meanings of the 12 TCIs are explained next:

(1) The type and dimension of the POC sets of the moving platform and the number of DOF of a PM reflect the basic function and performance requirement of the PM.

https://doi.org/10.1017/S0263574719001528 Published online by Cambridge University Press

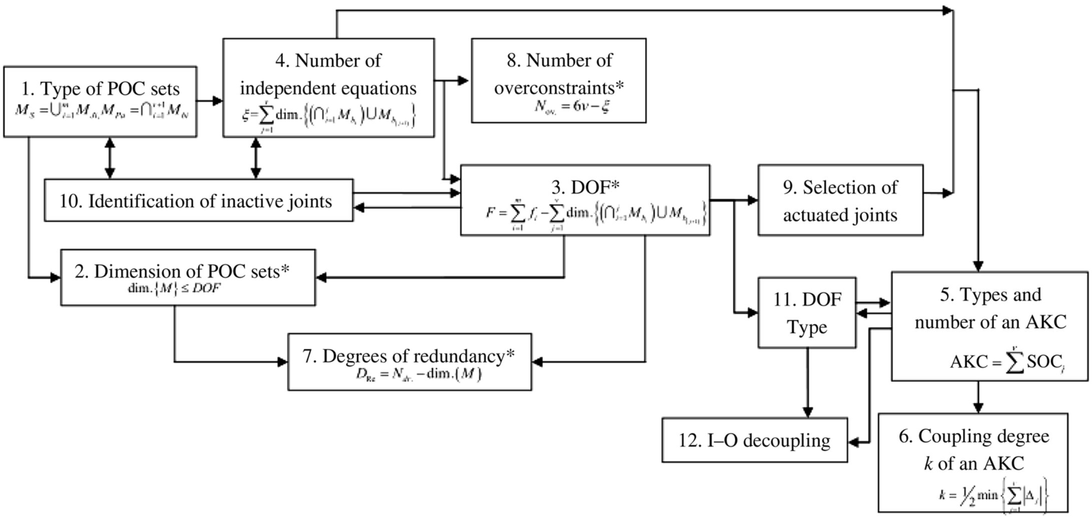

Fig. 6. Inherent correlations among the 12 TCIs for the ETP analysis.

(2) The number of independent loop displacement equations, the types and number of AKCs, the DOF types, coupling degree of an AKC and the identification of actuated joints of a PM reveal the basic topological characteristics and the complexity level of the kinematics and dynamics of the PM.
(3) The number of DOF, the DOF types, coupling degree of an AKC, degree of redundancy, the dimension of POC sets and I–O decoupling property of a PM indicate the complexity level of trajectory planning and motion control of the PM.
(4) The identification of inactive joints and the degree of redundancy can offer assistance for PM prototype design and manufacturing.

Moreover, we find that the 12 TCIs are interconnected with each other, with collective influence to topological, kinematic and dynamic properties of a PM. The inherent correlations among 12 TCIs are shown in Fig. 6.

Among the 12 TCIs, 5 are the most important for ETP of a PM (indicated with boxes 1, 3, 4, 5 and 6 in Figs. 5 and 6). The importance of the five TCIs will be illustrated at the end of Section 3.3. The other seven TCIs can be derived from these five TCIs.

It can be observed that each step of the ETP of a PM is accompanied with a specific calculation formulae and well-defined determination criteria, which make this ETP method clear and simple.

It is noted that the significance of the ETP for spatial PMs is greater than that of planar mechanisms since the TPs of planar mechanisms are relatively simple.

3. Illustrations of the ETP Method and Design Guidelines Derived from ETP Analysis

Six well-known industrial PMs and other 28 typical PMs are chosen to conduct an ETP analysis. Only partial details, such as calculation of POC, DOF, AKC, k, D_{Re}, N_{ov} and the description of I–O decoupling of Delta PM, are given in the following text due to the limited space. The TPs derived from the rest of the PMs will be listed in Tables III and IV. Furthermore, valuable design guidelines derived from the ETP analysis of these successful PMs will be presented.

In general, it is noted that when the type and the dimensions of a POC set for PM are discussed, an arbitrary point on the moving platform of a PM is chosen as the base point, that is, the origin of the movable coordinate system. Therefore, the analysis results are general.

3.1. ETP analysis for the existing PMs

3.1.1. 3-DOF Delta PM

Description The Delta PM shown in Fig. 7 consists of a moving platform, a base platform and three systematically placed hybrid chains connecting the moving platform and the base platform.

https://doi.org/10.1017/S0263574719001528 Published online by Cambridge University Press

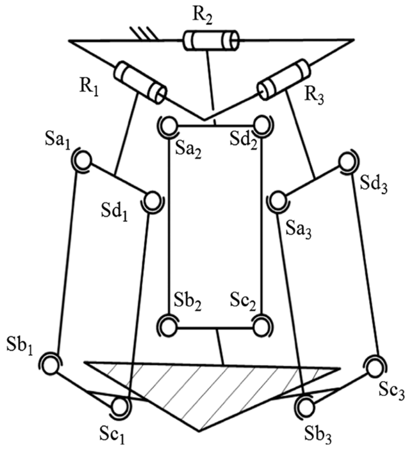

Fig. 7. Delta mechanism.

Each hybrid single-open-chain (HSOC) is connected to the base platform by an active revolute joint (R_1 or R_2 or R_3). Rigidly connected to the active joint is a parallelogram structure containing four spherical joints $S_{a_i}, S_{b_i}, S_{c_i}, S_{d_i}$ with $R_i//(a_id_i)(i=1,2,3)$. Here, $R_i//(a_id_i)$ means that the axes of R_i joint are parallel to the connecting line a_id_i between the spherical joints S_{ai} and S_{di}

Determination of POC

(1) Topological structure of this PM

The three HSOC$_s$ (or branches) have the same topological structure, which can be denoted as

$$\text{HSOC}\left\{-R_i\diamond(-S_{a_i}, S_{b_i}, S_{c_i}, S_{d_i})-\right\}, \quad (i=1,2,3).$$

The four connecting lines of the centres of the four spherical joints $S_{a_i}, S_{b_i}, S_{c_i}, S_{d_i}$ form a parallelogram, denoted by "◇". The other notations in the preceding formula can be found in refs. [6, 7]

(2) Determination of the POC set for the end-link of each branch

From Eq. (1) and the union operation rules, we have

$$M_{b_i} = \begin{bmatrix} t^1(\perp R_i) \\ r^1(\parallel R_i) \end{bmatrix} \bigcup \begin{bmatrix} t^1(\parallel\diamond(a_ib_ic_id_i)) \bigcup t^1(\perp(a_id_i)) \\ r^1(\parallel (a_id_i)) \bigcup r^1(\parallel b_id_i) \end{bmatrix} = \begin{bmatrix} t^3 \\ r^2(\parallel \diamond(R_i, (b_id_i))) \end{bmatrix}, i=1,2,3$$

It is noted that the rotation DOF about the line a_id_i (or b_ic_i) of a parallelogram structure is easy to be understood in the calculation of POC, ξ_{L_j} and DOF of the PM. However, the rotation DOF about diagonal line b_id_i (or a_ic_i) might be easily missed, it indeed exists and must to be considered in the calculation of the POC, ξ_{L_j} and DOF of the PM.

(3) Determination of the POC set of the sub-PM formed by the first and the second branch

From Eq. (2) and the intersection operation rules, we have

$$M_{pa(1\sim2)} = \begin{bmatrix} t^3 \\ r^2(\parallel\diamond(R_1, (b_1d_1))) \end{bmatrix} \bigcap \begin{bmatrix} t^3 \\ r^2(\parallel\diamond(R_2, (b_2d_2))) \end{bmatrix} = \begin{bmatrix} t^3 \\ r^1(\parallel(\diamond(R_1, (b_1d_1)) \bigcap \diamond(R_2, (b_2d_2))) \end{bmatrix}$$

(4) Determination of the POC set of the moving platform of the PM

https://doi.org/10.1017/S0263574719001528 Published online by Cambridge University Press

Because the joints R_1, R_2 and R_3 on the base are not parallel to each other, one can easily obtain from Eq. (2).

$$M_{pa} = M_{pa(1\sim2)} \bigcap M_{b_3} = \begin{bmatrix} t^3 \\ r^0 \end{bmatrix}$$

Therefore, the output motion of the moving platform shows three independent translations without rotations.

Calculation of DOF

(1) Determination of the number of independent displacement equations for the first loop, ξ_{L_1}

The first loop is formed by the first and the second branch, which also can be regarded as a sub-PM. According to Eq. (5b), we have

$$\xi_{L_1} = \dim.\left(\begin{bmatrix} t^3 \\ r^2(\| \diamond(R_1, (b_1d_1))) \end{bmatrix} \bigcup \begin{bmatrix} t^3 \\ r^2(\| \diamond(R_2, (b_2d_2))) \end{bmatrix}\right) = \dim.\left(\begin{bmatrix} \mathrm{t}^3 \\ r^3 \end{bmatrix}\right) = 6$$

The DOF of the sub-PM is calculated by Eq. (5a) as follows

$$F_{(1\sim2)} = \sum_{i=1}^{m} f_i - \sum_{j=1}^{1} \xi_{L_j} = 10 - 6 = 4$$

(2) Determination of the number of independent displacement equations for the second loop, ξ_{L_2}

The second loop is formed by the previous sub-PM and the third branch, which is already a PM. From Eq. (5b), we have

$$\begin{aligned} \xi_{L_2} &= \dim.(M_{pa(1\sim2)} \bigcup M_{b_3}) \\ &= \dim.\left(\begin{bmatrix} t^3 \\ r^1(//(\diamond(R_1, (b_1d_1)) \bigcap \diamond(R_2, (b_2d_2))) \end{bmatrix} \bigcup \begin{bmatrix} t^3 \\ r^2(//\diamond(R_3, (b_3d_3))) \end{bmatrix}\right) \\ &= \dim.\left(\begin{bmatrix} \mathrm{t}^3 \\ r^3 \end{bmatrix}\right) = 6 \end{aligned}$$

(3) Determination of the number of DOF of the PM

According to Eq. (5a), we have

$$F = \sum_{i=1}^{m} f_i - \sum_{j=1}^{2} \xi_{L_j} = 15 - (6 + 6) = 3$$

Comparing the dimension of the POC set of the moving platform and the number of DOF, it is found that the dimension of the POC set and the number of DOF are the same and equal to three, that is, $\dim.\{M_{Pa}\} = 3 = \mathrm{DOF}$, satisfying Eq. (4).

Therefore, three actuated joints must be assigned to this PM due to the fact that the PM has three DOFs. It is easily found that the three joints R_1, R_2 and R_3 on the base platform can be selected as the actuated joints according to the selection criterion of actuated joints, that is, index *No. 9*, illustrated in Section 2.1.9.

Identification of inactive joints Based on the identification criterion for inactive joints, that is, index *No. 10*, illustrated in Section 2.1.10, we have checked that the rotations about the diagonal lines $S_{bi}S_{di}$(or $S_{ai}S_{ci}$) (i = 1, 2, 3) are all inactive DOFs. Therefore, we must eliminate the three inactive rotational motions when in the following paragraph the constraint degree and the coupling degree are calculated.

Table II. Topological properties of Delta PM.

POC	DOF	ξ	N_{AKC}	k	v	D_{Re}	N_{ov}	I–O decoupling	m/n
$\begin{bmatrix} t^3 \\ r^0 \end{bmatrix}$	3	12	1	1	5	0	0	No	15/11

Here, N_{AKC} represents the number of AKC.

Calculation of the coupling degree

(1) Determination of SOC_1

Since there exist inactive rotational motions about the diagonal lines $S_{bi}S_{di}$(or $S_{ai}S_{ci}$) (i = 1, 2) in each of the identical branches that should be eliminated, the first loop formed by the first and the second branch has to be changed to

$$SOC_1 \left\{ -R_1//R^{(4S)}_{(//a_1d_1)} - P^{(4S)}_{(//\diamond(4S))} - P^{(4S)}_{(\perp a_1d_1)} - P^{(4S)}_{(\perp a_2d_2)} - P^{(4S)}_{(//\diamond(4S))} - R^{(4S)}_{(//a_2d_2)}//R_2- \right\}$$

Using the same procedure as stated in the calculation of the DOF, we calculate that the number of independent displacement equations for the first loop is $\xi_{L_1} = 5$.

(2) Calculation of the constraint degrees Δ_1 of SOC_1

According to Eq. (8), we get

$$\Delta_1 = \sum\nolimits_{i=1}^{m_1} f_i - I_1 - \xi_{L_1} = 8 - 2 - 5 = +1$$

(3) Determination of SOC_2 and calculation of constraint degrees Δ_2

The second loop formed by the previous sub-PM and the third branch can be determined after the elimination of the inactive rotational motions about the diagonal line $S_{b3}S_{d3}$(or $S_{a3}S_{c3}$).

$$SOC_2 \left\{ -R_3//R^{(4S)}_{(//a_3d_3)} - P^{(4S)}_{(//\diamond(4S))} - P^{(4S)}_{(\perp a_3d_3)} - \right\}.$$

Using the same procedure as in the calculation of the DOF, we calculate the number of independent displacement equations for the second loop with $\xi_{L_2} = 4$.
Then we obtain according to Eq. (8)

$$\Delta_2 = \sum_{i=1}^{m_2} f_i - I_2 - \xi_{L_2} = 4 - 1 - 4 = -1$$

Determination of the AKC and its coupling degree As this PM contains only one AKC the coupling degree of the AKC is obtained from Eq. (9)

$$k = \frac{1}{2}\sum_{j=1}^{v} |\Delta_j| = \frac{1}{2}(|+1| + |-1|) = 1$$

Since the coupling degree of the AKC is 1, the forward kinematics solution of the PM can be obtained easily using the one-dimension search method.

TPs of Delta PM With the main TCIs derived earlier, other TCIs, like D_{Re}, N_{ov} , *I–O* decoupling, can be easily derived. All TCIs are displayed in Table II.

In order to increase the workspace of the Delta PM, Tsai has designed a new mechanism by replacing the 4S parallelogram structure with a 4R parallelogram structure.[16] Moreover, Wenger proposed the Orthoglide robot[17] that evolved from the Tsai mechanism by replacing the revolute

https://doi.org/10.1017/S0263574719001528 Published online by Cambridge University Press

Table III. Topological properties of the six well-known PMs.

	Mechanism	POC	DOF	ξ	N_{AKC}	k	v	N_{ov}	I–O decoupling	m/n
1	3-DOF Delta[8]	$\begin{bmatrix} t^3 \\ r^0 \end{bmatrix}$	3	12	1	1	5	0	No	15/11
2	3-DOF Tricept[4]	$\begin{bmatrix} t^1 \\ r^2 \end{bmatrix}$	3	18	1	2	3	0	No	11/9
3	3-DOF Exechon[21]		3	10	1	2	2	2	No	9/8
4	3-DOF Z3[20]		3	12	1	1	2	0	No	9/8
5	4-DOF H4[22]	$\begin{bmatrix} t^3 \\ r^1 \end{bmatrix}$	4	6	1	2	3	0	No	22/16
6	6-DOF Stewart[24]	$\begin{bmatrix} t^3 \\ r^3 \end{bmatrix}$	6	30	1	3	5	0	No	18/14

joints with prismatic joints and changing the organization of the three chains.[18] Obviously, the *DOF, POC* sets and coupling degree k of these revised mechanisms remain the same as those of the original Delta.

We have also performed detailed ETPs for five other well-known PMs.[19–24] Table III lists their derived TPs.

3.1.2. Other typical PMs. In addition to these 6 well-known PMs, additional 28 typical PMs[18,25–40] from 2-DOF to 6-DOF were examined with the ETP analysis. The 28 typical PMs designed and analysed by different researchers are selected from a large number of references. The ETP results of the 28 typical PMs can be found in refs. [25, 41]. Only 1 of 12 TCIs, namely the coupling degrees k which is very important, is listed in Table IV to extract some valuable design guidelines.

3.2. Analysis results and knowledge obtained from ETP of the existing PMs

Results from the ETP analysis of a large number of PMs led to some important design knowledge listed earlier. Among the investigated manipulators are six well-known PMs having 3-DOF PMs like the Delta, the Tricept, the Exechon and the Z3, the 4-DOF PMs H4 and the Gough–Stewart platform with 6-DOF. Furthermore, 28 typical PMs were studied, 6 of them are 2-DOF PMs, 11 are 3-DOF PMs, 6 are 4-DOF PMs, 4 are 5-DOF PMs and 1 is a 6-DOF PM.

(1) Among the six well-known PMs, three PMs, the Delta, Exechon and Z3, have a coupling degree of 1 and two others (i.e., Tricept and H4) have a coupling degree of 2. The sixth one, the Gough–Stewart platform, has a coupling degree of 3. This indicates that the PMs with coupling degree 1 are widely used.

(2) Among the 28 typical PMs, 6 of these PMs have a coupling degree 0, 12 PMs have a coupling degree of 1, 9 PMs have a coupling degree of 2 and 1 PM has a coupling degree of 3. Obviously, the PMs with coupling degrees 0 and 1 are widely used. The popularity of low coupling degree manipulators is due to the easy kinematic and dynamic analysis of these PMs. While few PMs have zero coupling degree, these devices have all been successfully adopted by industry. This should motivate researchers to invent new PMs with zero coupling degree.

(3) I–O motion decoupling is a very important index that reflects the simplicity of the trajectory planning and motion control. But the six existing well-known PMs are all not I–O motion decoupled. This should motivate researchers to improve the I–O motion decoupling for PMs.

(4) The degrees of redundancy D_{re} of all six existing PMs are zero. The number of overconstraint N_{ov} for most PMs is zero except 3-DOF Exechon whose $N_{ov} = 2$. Larger overconstraint values result in greater susceptibility to manufacturing errors of PMs.

3.3. Guidelines for design of PMs

Furthermore, the results from the ETP for 6 well-known PMs and 28 typical PMs led to some valuable design guidelines for the design of novel PMs:

https://doi.org/10.1017/S0263574719001528 Published online by Cambridge University Press

Table IV. Important topological properties of successful PMs.

DOF	Six well-known PMs	Twenty-eight typical PMs
2		Diamond (2T, $k = 0$)[17] 2-RRC+1-RRR (2T, $k = 1$)[40] 2-RPR+1-RP (1T1R, $k = 0$)[40] Bicept (1T1R, $k = 1$)[28] RR+RPS+SPS (2R, $k = 0$)[40] Omni-Wrist III (2R, $k = 1$)[29]
3	Delta (3T, $k = 1$)[8] Tricept (1T2R, $k = 2$)[26] Exechon (1T2R, $k = 1$)[21] Z3 (1T2R, $k = 1$)[20]	TriVariant (1T2R,$k = 1$)[24] 3-RRC (3T, $k = 1$)[5] 3-UPU (3T, $k = 2$)[25] 2-SPS+1-RPR (2T1R, $k = 1$)[40] 3-SPS+1-RPR (2T1R, $k = 2$)[18] PS+PRS+PSS (1T2R, $k = 0$)[6] 3-RSR (1T2R, $k = 1$)[32] 3-RPS (1T2R, $k = 1$)[24] 3-RRR (3R, $k = 1$)[26] 3-RRS (3R, $k = 1$)[34] 3-UPU (3R, $k = 2$)[33]
4	H4 (3T1R, $k = 2$)[22]	4-UPU (3T1R, $k = 2$)[24] 2-RPS+2-SPS (2T2R, $k = 1$)[26] 4-R (CRR)(2T2R, $k = 2$)[24] 2-SPS+PS+SPS (1T3R, $k = 0$)[30] 3-PTS-PRT (1T3R, $k = 2$)[25] Linear Delta Robot[18]
5		4-SPS+RRUR (3T2R, $k = 2$)[37] 4-SPS+PPPU (3T2R, $k = 2$)[37] 2-SPS+RPR+RPS+SPS (2T3R, $k = 0$)[38] 3-PR (RRR)(2T3R, $k = 1$)[39]
6	Gough–Stewart (3T3R, $k = 3$)[24]	6-RUS (3T3R, $k = 3$)[4]

(1) Lower-DOF PMs, especially 2-DOF and 3-DOF PMs, can be connected with one or two rotational or translational DOF on a moving platform and constitute hybrid mechanisms. These hybrid mechanisms have the benefits of both parallel and serial mechanisms. They are more suitable for industrial applications. Based on this, we developed five novel PM-based prototypes used in customized applications.

(2) I–O motion decoupling is a useful property for the simplicity of trajectory planning and motion control algorithms. Therefore, the I–O motion decoupling property should be considered when we design PMs.

(3) For a PM with a driven passive branch, researchers can reduce its coupling degree k from 2 to 1 or from 1 to zero by converting the driven passive branch into a driving one. For example, a TriVariant with a coupling degree 1 is derived from Tricept with a coupling degree of 2, but its POC and DOF are unchanged.[25] This design approach also provides a method to optimize the topological structure of existing PMs.

(4) PMs with more DOFs involve higher numbers of independent loop displacement equations, which generally lead to higher coupling degree k.

In short, the application of ETP analysis to 6 well-known and 28 typical PMs identified five most interesting TPs, that is, DOF, POC sets, number of independent displacement equations ξ, coupling degree k, as well as types and number of AKC. Hereby, DOF analysis enhances existing knowledge about the performance of input and control. POC sets analysis helps researchers select output motion

https://doi.org/10.1017/S0263574719001528 Published online by Cambridge University Press

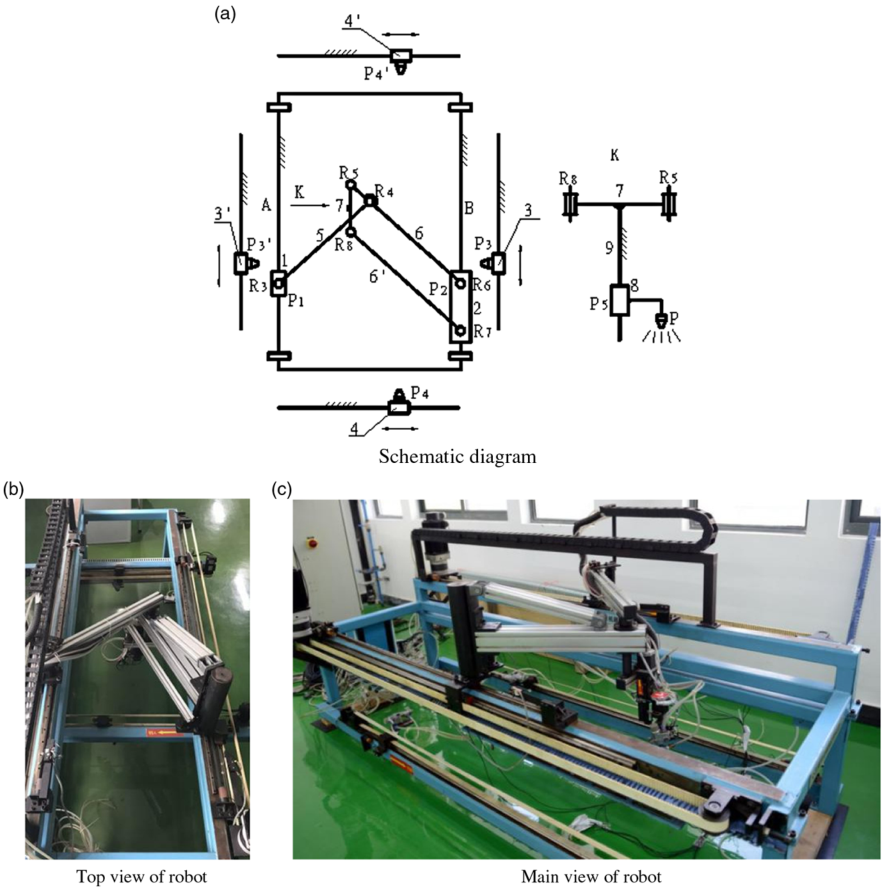

Fig. 8. A practical 5-DOF decoupling hybrid spraying robot.

types satisfying the basic functions and design requirements. In addition, the number of independent displacement equations ξ, the coupling degree k and the type and number of AKCs involve the interdependent relationship between the kinematic or dynamic variables of each loop, and facilitate the assessment of the complexity level of kinematics and dynamics solutions.

4. Applications

Both, the design knowledge obtained from the ETP analysis of the existing PMs stated in Section 3.2 and the design guidelines for the design of PMs stated in Section 3.3 are very important, are useful and have been really applied in our new PM designs. Here we illustrate only the procedure of a 5-DOF decoupled hybrid spraying robot[42] in detail.

4.1. Determination of POC and DOF based on task analysis

A 5-DOF decoupled hybrid spraying robot has been developed for a coating company. The spraying target is a cubic object that has five surfaces to be sprayed, one of which is a relatively large main rectangle surface and the others are four smaller surfaces, that is, the left and right lateral surfaces, as well as the front and back surfaces. The spraying speed of over 1 m/s is demanded for high production efficiency. Therefore, 5-DOFs are needed to accomplish the task. Further, a hybrid robot with good I–O motion decoupling property is the most promising choice according to the design guidelines 1 and 2 in Section 3.3.

4.2. Design of a 5-DOF decoupling spraying robot

First, we allocate 5-DOF to three independent mechanisms as shown in Fig. 8(a). They are:

① A spraying mechanism for the main large rectangle surface. As it can be seen in Fig. 8(a), a 2-DOF PM module composed of a closed planar chain P_1-R_3-R_4-R_6-P_2 driven by two sliders 1

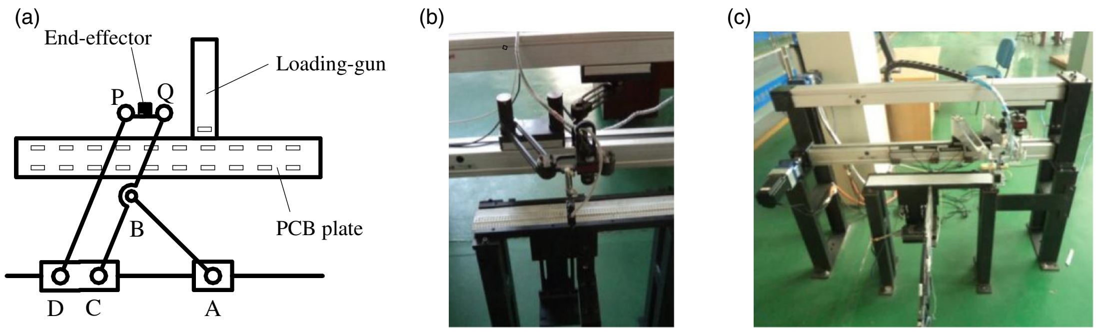

2-DOF 2T PM with $k = 0$ 2- DOF 2T PM ⊕ 2-dof Z-θ system 4- DOF Prototype

Fig. 9. 4-DOF hybrid robot for SMT.

and 2 is adopted. Further, a 4R parallelogram is constructed by adding a planar open kinematic chain R_5-R_8-R_7 to the link 6 and slider 2, which ensures that the pose of link 7 is unchanged. A 1-DOF translational mechanism, consisting of the linear guide 9 and the slider 8 connected to link 7, is vertical to the moving plane of link 7. The structure outputs a translation along the vertical direction to the moving plane of link 7.

② A spraying mechanism for the left and right lateral surfaces. The spray guns P_3 and P_3' are driven by two 400 W servo-motors and move along the two horizontal guide rails 3 and 3'.

③ A spraying mechanism for the front and back surfaces. The spray guns P_4 and P_4' are also driven by two 400W servo-motors and move also along two horizontal guide rails 4 and 4' that are perpendicular to the guide rails 3 and 3'.

Figure 8(b) and 8(c) shows the developed prototype of 5-DOF decoupled hybrid spraying robot. During designing of the 5-DOF hybrid spraying robots, two design guidelines described in Section 3.3, a simpler 2-DOF PM integration module with coupling degree k zero and the I–O motion decoupling property, have been adopted.

Inspired by the design knowledge and design guidelines obtained from the ETP method introduced in this article, we have developed other novel PM-based prototypes used in customized applications in addition to the design example of the 5-DOF decoupling hybrid spraying robot. For example, a novel 4-DOF robot for SMT (surface mount technology) was invented[43] that adopts a 2-DOF zero coupling degree (two pure translations) PM (Fig. 9), and a novel 5-DOF hybrid test platform for a photovoltaic product[44] was invented that adopts a 3-DOF 2T1R (two translation and one rotation) PM with $k = 0$ and I–O decoupled, both of which are not described in detail due to the lack of space in this article.

5. Conclusions

The goal of the article was to address the importance of the ETP analysis of PMs and to express and evaluate TPs through TCI. This article presented three contributions. First, a general and effective ETP method of PMs including 12 TCIs was proposed. Based on this systematic ETP method, the key TPs of any PMs can be discovered, thereby facilitating additional topological optimization and improvement. Second, the ETP results provide some important knowledge and valuable guidelines for the design of PMs, based on which some novel and practical multi-DOF decoupled hybrid robots with low coupling degree, 0 or 1, have been developed. Third, some important design knowledge and guidelines derived from ETP of 6 well-known and 28 typical PMs have been found. For example,

① 2-DOF and 3-DOF PMs can be used as standalone devices or integration modules for hybrid robots that may result in the I–O motion decoupling property.

② PMs with coupling degrees of 0 and 1 are computationally more efficient as less-implicit equations have to be iteratively solved.

③ For PMs with a driven passive limb, researchers can reduce their coupling degree from 2 to 1 or from 1 to 0 through converting the driven passive branch into a driving branch. This design approach provides a method to optimize the topological structure of existing PMs.

The ETP method introduced in this article enhances the theoretical analysis, design and practical applications of PMs. It enables researchers to improve existing PMs and to design many novel PMs. It is encouraged for other researchers to include ETP in the analysis, design and development of PMs.

Acknowledgements
This research was possible thanks to support from the National Natural Science Foundation of China (Grants No. 51975062, No. 51475050 and No. 51375062). The authors express their gratitude to Prof. Manfred Husty, Mr. Florian Simroth and Mr. Shaobin Tao for their kind assistance.

References

1. A. Frisoli, F. Checcaci and F. Salsedo, "Synthesis by screw algebra of translating in-parallel actuated mechanisms," *Adv. Rob. Kinematics*, 433–440 (2000).
2. X. Kong and C. M. Gosselin, *Type Synthesis of Parallel Mechanisms* (Springer, Berlin, Heidelberg, 2007) pp. 45–53.
3. Q. C. Li, Z. Huang and J. M. Herve, "Type synthesis of 3R2T 5-DOF parallel mechanisms using the lie group of displacements," *IEEE Trans Robotic Autom*. **20**(2), 173–180 (2004).
4. G. Gogu, *Structural Synthesis of Parallel Robots. Part 1:Methodology* (Springer, Netherlands, 2008).
5. Q. Jin and T.-L. Yang, "Theory for topology synthesis of parallel manipulators and its application to three dimension translation parallel manipulators," *ASME J Mech. Des.* **126**(4), 625–639 (2004).
6. T.-L. Yang, A.-X. Liu, Q. Jin, Y.-F. Luo, H.-P. Shen and L.-B. Hang, "Position and orientation characteristic equation for topological design of robot mechanisms," *ASME J. Mech. Des.* **131**(2), 021001-1-17 (2009).
7. T.-L. Yang, A.-X. Liu, H.-P. Shen, Y.-F. Luo, L.-B. Hang and Z.-X. Shi, "On the correctness and strictness of the position and orientation characteristic equation for topological design of robot mechanisms," *ASME J. Mech. Rob.* **5**(2), 021009 (2013).
8. T. L. Yang, A. Liu, H. Shen, L. Hang, Y. Luo and Q. Jin, "General Method for Topology Design of Parallel Mechanisms," **In**: *Topology Design of Robot Mechanisms* (Springer, Singapore, 2018) pp. 177–206.
9. H. Shen, H. Yin, Z. Wang, T. Huang, J. Li, J. Deng and T. Yang, "Research on forward position solutions for 6-sps parallel mechanisms based on topology structure analysis," *Chin. J. Mech. Eng.* **49**(21), 70–80 (2013).
10. H. Shen, L. Yang, Q. Meng and H.-B. Yin, "Topological Structure Coupling-Reducing of Parallel Mechanisms," *Proceedings of 2015 IFToMM World Congress,* Taipei (2015) 10.25–29.
11. T.-L. Yang and D.-J. Sun, "A general DOF formula for parallel mechanisms and multi-loop spatial mechanisms," *ASME J. Mech. Rob.* **4**(1), 011001 (2012).
12. Z. Xiaorong, Y. Tingli, Y. Sen, H. Jun and S. Huiping, "Computer-Aided Analysis for Topological Structure of Parallel Mechanisms," *The 8th IEEE International Conference on Cybernetics and Intelligent Systems (CIS) and the 8th IEEE International Conference on Robotics, Automation and Mechatronics (RAM)*s, Ningbo, China, **11**, 19–21(2017).
13. M. Carricato and V. Parenti-Castelli, "A novel fully decoupled two-degrees-of-freedom parallel wrist," *Int. J. Rob. Res.* **23**(6), 661–667 (2004).
14. O. Altuzarra, M. Loizaga and C. Pinto, "Synthesis of partially decoupled multi-level manipulators with lower mobility," *Mech. Mach. Theory* **45**(1), 106–118 (2010).
15. G. Legnani, I. Fassi, H. Giberti, C. Cinquemani and D. Tosi, "A new isotropic and decoupled 6-DOF parallel manipulator," *Mech. Mach. Theory* **58**, 64–81 (2012).
16. L. W. Tsai, "Kinematics of a 3-DOF Platform with Three Extensible Limbs," **In:** *Recent Advance in Robot Kinematics* (J. Lenarcic and V. H. Parenti-Castelli, eds.) (Kluwer Academic Publishers, Boston, 1996), pp. 401–410.
17. P. Wenger and D. Chablat, "Kinematic Analysis of a New Parallel Machine Tool: The Orthoglide," **In:** *Advances in Robot Kinematics* (J. Lenarcic and M. L. Stanisic, eds.) (Kluwer Academic Publishers, Boston, 2000), pp. 305–314.
18. E. Baran, O. Ozen, D. Bilgili and A. Sabanovic, "Unified kinematics of prismatically actuated parallel delta robots," *Robotica* **37**(9), 1513–1532 (2019). doi:10.1017/S0263574719000092.
19. T. Huang, Z. X. Li, M. Li, D. G. Chetwynd and C. M. Gosselin, "Conceptual design and dimensional synthesis of a novel 2-DOF translational parallel robot for pick-and-place operations," *ASME J. Mech. Des.* **126**(3), 449–455 (2004).
20. W. Dan, F. Rui and C. Wuyi, "Performance enhancement of a three-degree-of-freedom parallel tool head via actuation redundancy," *Mech. Mach. Theory* **71**, 142–162 (2014).
21. Z. M. Bi and Y. Jin, "Kinematic modeling of Exechon parallel kinematic machine," *Rob. Comput. Integr. Manuf.* **27**(1), 186–193 (2011).
22. K. E. Neumann, Robot. *US Patent*, 1988, **5**, No: 4732525.
23. F. Pierrot, High-Speed Parallel Robot with Four Degrees of Freedom, US20090019960A1. (2009).
24. D. Stewart, "A platform with six-degree-of-freedom," *Proc. Inst. Mech. Eng.* **180**(15), 371–378 (1965).
25. H. B. Yin, *Topological Structure and Kinematics Study of Parallel Mechanisms* (Changzhou University, Changzhou, 2014).
26. F. Gao, J. L. Yang and Q. D. Ge, *GF Set Theory for Type Synthesis of Parallel Mechanisms* (Science Press, Beijing, 2011).

27. X. J. Liu and J. Wang, *Parallel Kinematics – Type, Kinematics and Design* (Springer, Berlin, Heidelberg, 2014).
28. Q. Li, Z. Chen, Y. Han and Q. Chen, Intersectional 2-dof Parallel Mechanisms, *China patent*, No: 201010153843.7 (2010).
29. M. X. Wang, P. F. Wang, Z. M. Song, X. M. Zhao and T. Huang, "Static rigidity analysis for a 4-dof hybrid robot," *Chin. J. Mech. Eng.* **47**(15), 9–16 (2011).
30. M. Rosheim, Robotic Manipulator U.S. 5979264. 1999–10
31. L. W. Tsai, Multi-Degree-of-Freedom Mechanisms for Machine Tools and the Like. *U.S. Patent* No. 5656905 (1997).
32. H. S. Kim and L. W. Tsai, "Evaluation of a Cartesian Parallel Manipulator," **In:** *Advances in Robot Kinematics* (J. Lenarcic and F. Thomas, eds.) (Kluwer Academic Publishers, Dordrecht, 2002), pp. 21–28.
33. R. Di Gregorio, "Kinematics of the 3-RSR wrist," *IEEE Trans. Rob.* **20**(4), 750–753 (2004).
34. M. Karouia and J. M. Herve, *A Three-dof Tripod for Generating Spherical Rotation, Advances in Robot Kinematics* (Kluwer Academic Publishers, Boston, 2000), pp. 395–402.
35. Y. F. Fang and L. W. Tsai, "Structure synthesis of a class of 3-dof rotational parallel manipulators," *Trans. Rob. Autom.* **20**(1), 117–121 (2004).
36. H. Zhen, Z. Yan and L. Jingfang, "Kinetostatic analysis of 4-R(CRR) parallel manipulator with overconstraints via reciprocal-screw theory," *Adv. Mech. Eng.* **2**, 1–11 (2010).
37. Z. Dimiter and M. Gosselin, "A family of new parallel architectures with four degrees of freedom," *Electron. J. Comput. Kinematics* **1**(1), 57–66 (2002).
38. J. S. Wang and L. Z. Ma, "Kinematic analysis of novel five-DOF parallel mechanism," *J. Jiangsu Univ.* **25**(2), 153–156 (2004).
39. W. M. Li and F. Gao, "The Structure Design and Analyses of Parallel Milling Machine with 5-DOF," *Modular Mach. Tool Automa. Manuf. Tech.* (3), 3–4 (2004).
40. H. L. Chen, Y. F. Luo, J. X. Li and Z. X. Shi, "Research on a novel 2T3R parallel manipulator," *Mach. Tool Hydraul.* **35**(11), 23–24 (2007).
41. H. Shen, H. Yin, J. Li and J. Deng, "Position and orientation characteristic based method and enlightenment for topology characteristic analysis of typical parallel mechanisms and its application," *Chin. J. Mech. Eng.* **49**(21), 71–80 (2013).
42. J. Li, D. Zhao, H. Shen and J. Deng, "Design of 5-axes hybrid robot with multi-spray guns for collaborative spraying," *Trans. Chin. Soc. Agric. Mach.* **43**(4), 216–220 (2012).
43. H. B. Zhao, *The Research and Application of Hybrid Robot Mechanism* (Changzhou University, Changzhou, 2012).
44. W. Wang, *Design and Analysis for Parallel /Hybrid Mechanisms Used for Optical Inspection Platforms* (Changzhou University, Changzhou, 2012).